Fall 2019

Frequency Control of Laser Generated Ultrasonic Waves

Roberto Alva
alva2@iastate.edu

FREQUENCY CONTROL OF LASER GENERATED ULTRASONIC WAVES

by

Roberto Alva

A Creative Component submitted to the Graduate Faculty

In partial fulfillment of the requirements for the degree of

MASTERS OF SCIENCE

Major: Electrical Engineering

Program of Study Committee:

Timothy Bigelow, Major Professor

Department of Electrical and Computer Engineering,

Iowa State University

Ames, IA

Table of Contents

List of Figures

List of Tables

ABSTRACT

In this paper, the effects of varying the spot size of a high-power laser on the generation of acoustic waves are explored. The study simulated the interaction of the laser with a stainless-steel sample away from the ablation region. The simulations provided a set of data for the selection of a laser spot size that is needed for detecting pores in additive manufacturing samples. The simulations show that as the spot size of the laser decreased, the frequency would increase at a rate that is approximately the inverse of the spot size. Due to the desire to detect smaller flaws and from the knowledge that the spot size has a large variation near the focal point, it would be beneficial to understand the effects that occur due to the variation of the spot size, particularly in regards to the frequency content provided by a single pulse.

Keywords: Beam spot, laser ultrasonics, ultrasound frequency, non-destructive evaluation

1. INTRODUCTION

In order to better set up and interpret the results obtained using laser ultrasonic methods, a study was conducted to see what happens to the ultrasonic signal generated when the spot size changes. This was of particular importance when performing measurements because it allows the user better quality control. Currently, most laser ultrasonic tools are specified with a given frequency span of 100's kHz to 10's of MHz [1,2,3]. This paper will mostly focus on the vertical velocity of the wave generated along the surface of a material for the purpose of examining the effects that occur due to the variation of the spot size.

1.1 Model

For this experiment, COMSOL was used to generate several results based on the spot size of the incident laser. The laser intensity incident on the surface of the material was defined as

$$I = I_o e^{-\frac{2r^2}{r_{spot}^2}} \quad [1]$$

where r_{spot} was defined as the radius where $I = I_o * e^{-2}$ and the modulation of the laser pulse was defined in by Figure 1.

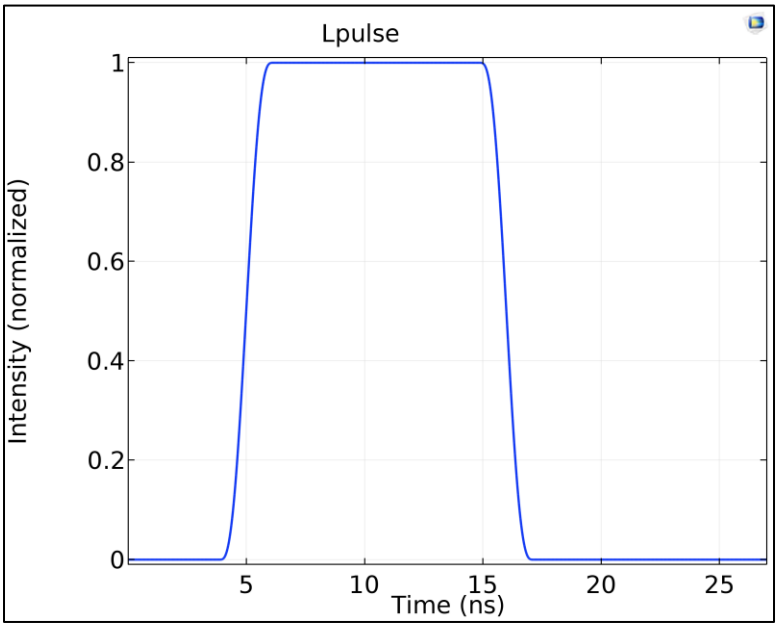

Figure 1: Laser pulse width used in the experiment.

Table 1: Material specific properties used for a steel sample.

Material Property	Value
Density	7750 $kg\ m^{-3}$
Poisson Ratio	0.30406
Elastic Modulus	196.76 GPa
Shear Modulus	75.442 GPa
Radiant Heat Emissivity	0.8
Specific Heat	475 J $(kg\ C)^{-1}$
Thermal Diffusivity	$1.2088 * 10^{-5}\ m^2\ s^{-1}$
Pulsed Laser Energy	3.5272 μJ
Melting Point	67195 $W\ m^{-1}$

The material used was metal with no pores and has a smooth surface. The top surface where the laser pulse initially hits was modeled using the boundary conditions for a free surface. In addition, this surface is modeled with more elements in order to properly take into account the expansion of the metal due to laser heating. The samples of the models were taken at half the domain space on the surface, where the domain was defined as the distance needed for the longitudinal wave to be sufficiently separate from the Rayleigh wave. This was of particular importance to ensure that the two signals do not interfere with each allowing for the Rayleigh wave to be easily separated from the longitudinal wave.

Table 2: The laser spot size diameters used in the model to generate the elastic waves.

Spot Size	50 µm	100 µm	200 µm	400 µm	800 µm	1000 µm	1600 µm	2000 µm

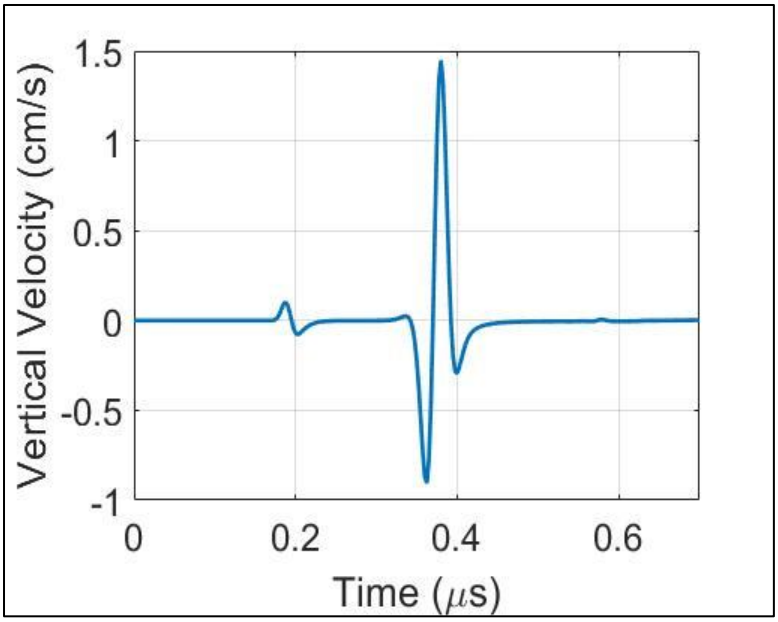

Figure 2: Vertical velocity of the surface wave for a laser spot size of 50 um.

Based on Figure 2, it could be seen that two different waves were generated. The Rayleigh wave, in particular, had a relatively strong signal compared to the longitudinal wave. This was useful for the purpose of measuring defects on the surface of a material. However, it was also important that the frequency generated was useful for the purposes of non-destructive testing. In particular, a larger frequency will allow for the detection of smaller pores and defects. Whereas smaller frequencies will be able to penetrate deeper into the sample.

2. Simulation Results

2.1 Frequency Response

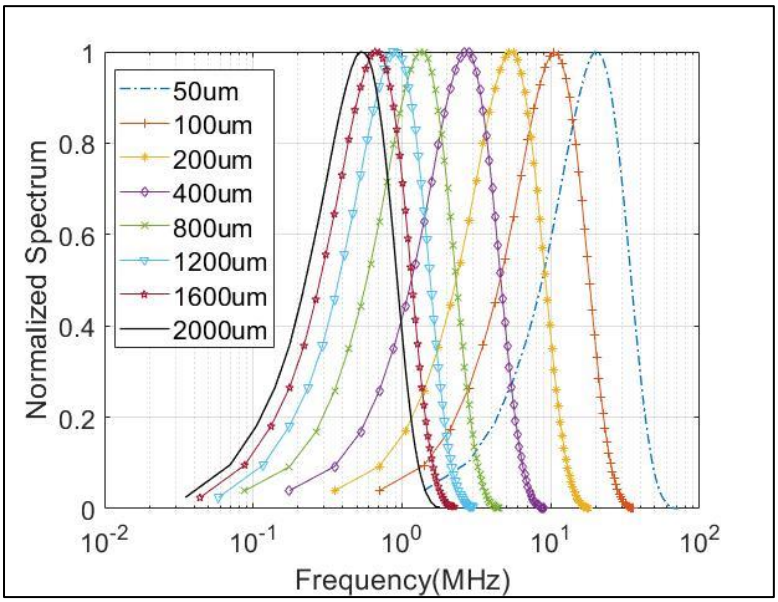

Figure 3: The normalized magnitude of the frequency response for a Rayleigh wave of varying incident spot sizes.

Figure 3 shows the frequency response of all the spot sizes used in the model. It can be seen that at large spot sizes the frequency content does not change as much as the smaller spot sizes. This was important when taking samples. Also, for a laser, the intensity the material sees before absorption can be approximated with a Gaussian profile

$$I = I_o e^{-2\left(\frac{r}{w(z)}\right)^2} \quad [2]$$

$$w(z) = w_o \sqrt{1 + \left(\frac{z}{z_o}\right)^2} \quad [3]$$

$$z_o = \frac{\pi w_o^2}{\lambda} \quad [4]$$

where w_o was the spot size radius and $w(z)$ was the spot size radius as it propagates along the z-direction. Assuming very little variation in the viewing angle at normal incidence, then it would be best to keep the receiver and the laser ultrasonic generating laser within the Rayleigh range of the laser to maximize the ultrasonic frequency. More specifically, in regards to NDT, a large spot

size at a large enough frequency would be desired such that the Rayleigh range is much larger than the variations in distance caused by the motors and the surface variations of the sample.

Another area of importance, the receiver used should have a good spatial resolution. In the simulations, all data was measured at a point away from the source. So, for a laser-based receiver, it would be important that the systems incident beam on the sample be relatively much smaller than the wavelength of the Rayleigh and shear waves. The benefit of this is that data requirements are relatively low and it is relatively inexpensive relative to imaging systems. However, this comes with challenges in regards to alignment and spot size stability of the laser heating source and the receiver system. So instead a large spot size may be used. In regards to the receiver system, the sampled area is illuminated and the light reflected is collimated onto a camera with a relatively small area and high pixel density. A benefit of the larger spot size would be that it is more stable, assuming the lens has a large focal spot size. However, using this method may then limit the temporal resolution, increase data requirements, and significantly increase computational requirements for real-time measurements.

2.2 Spot Size Relation

From the simulations, a relationship was determined between the spot size incident on the sample and the peak frequency detected.

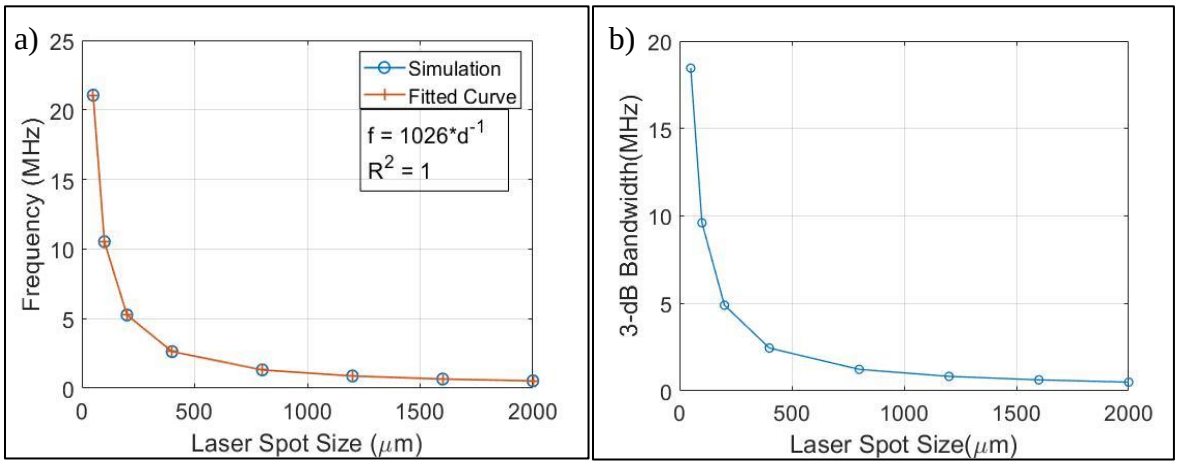

Figure 4: Peak Frequency and 3-dB bandwidth in relation to the spot size.

In Figure 4, the frequency generated from the model was fitted with a curve with respect to the spot size. The curve can be made by taking several data points and performing linear regression.

An assumption was made such that the frequency was dependent on a constant multiplied with the spot size to some exponent n and then taking the logarithms of both sides.

$$\log(f_{peak}) = c + nlog(d) \quad [5]$$

From the data, the computed values for c and n were 1026 and -1 respectively. When performing numerical simulations, this may prove useful for determining the correct spot size and laser needed for the experiment. Numerical simulations may take precious time and resources. So rather than guessing a spot size, one can simply run a model first for a given material and then input the peak frequency and spot size into the expected model and calculate the parameter c. Since the smallest feature that can be detected is dependent on the size of the wavelength, the wavelength desired can be calculated by using the expected material parameters of the sample to determine the velocity of the waves. The wavelength preferred for the feature can then be used in conjunction with the velocity to find the appropriate frequency. Based on the model, the expected RMS error of the calculated frequency was $1.6 * 10^{-9}$ for the given range of spot sizes.

2.3 Rayleigh Wave Attenuation

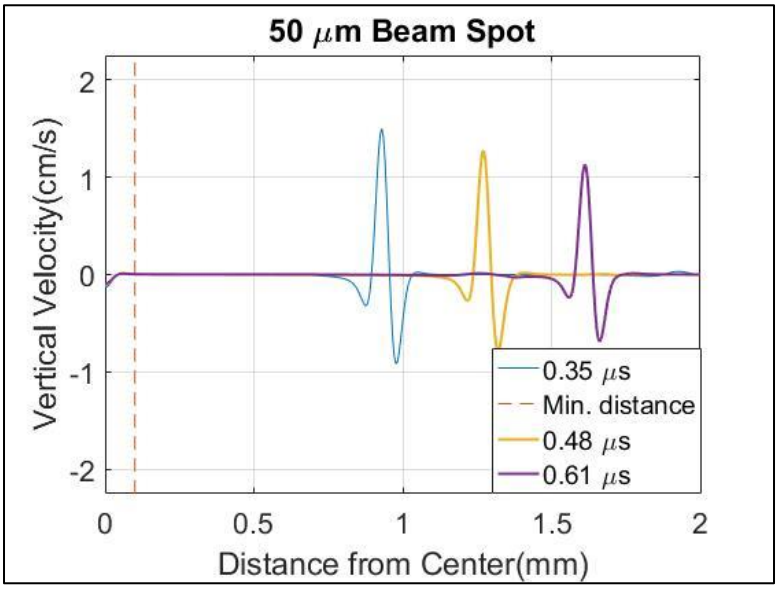

Figure 5: Region of uncertainty due to thermal expansion and cooling.

In Figure 5, there exists a region in the incident area where the area is still cooling down. Behind the dotted line, the velocity remains negative and slowly decays in amplitude. For the purpose of sampling flaws via the Rayleigh wave, the sampling spot should be placed at least 2 times the

radius of the spot size plus 2 times the radius of the sampling beam to ensure that none of the transient effects at the center alter the results.

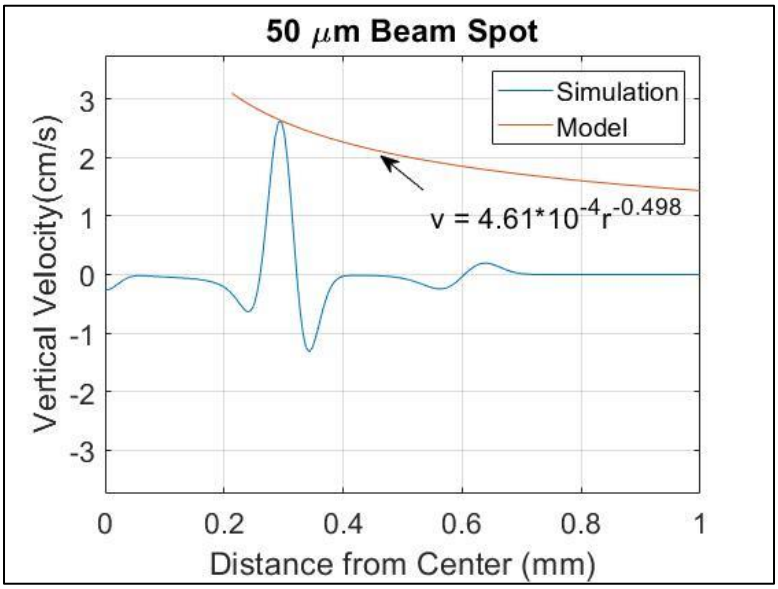

Figure 6: Strength of the surface wave as it propagates along the surface.

Lastly, the Rayleigh wave attenuation was determined to decrease inversely with the square root of the distance. Assuming the wave is sufficiently far away from the center, an appropriate range may be calculated such that the signal is sufficiently strong enough to be detected by the detector. This will depend on the detector, but given the minimum detectable signal at a given frequency, one can then determine the maximum distance from the center the Rayleigh wave can be inspected. Unlike the frequency model, the constant relating the peak vertical velocity and the distance does not remain the same for different spot sizes.

2.4 Variations in Pore Diameter and Depth

It can be determined from Figure 7 that as the spot size is decreased, the amplitude changes increase for each pore size. In addition, the figures demonstrate that the wave generated by the smaller spot sizes interact more strongly with pore diameters less than 100 μm compared to the larger spot sizes. From Figure 3, it is apparent that the reason for this is due to the high-frequency content generated by the smaller spot size. Also, if the focus is shifted towards the center of the spot, the changes in the amplitude are much stronger. This will be particularly useful when noise can be introduced by the detection system.

a)

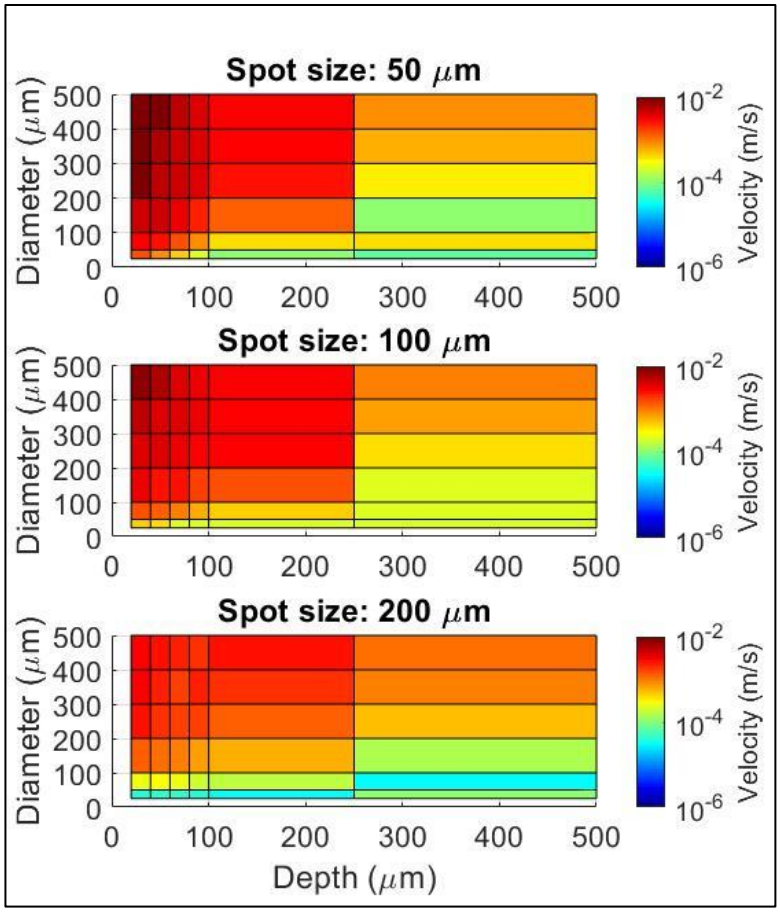

b)

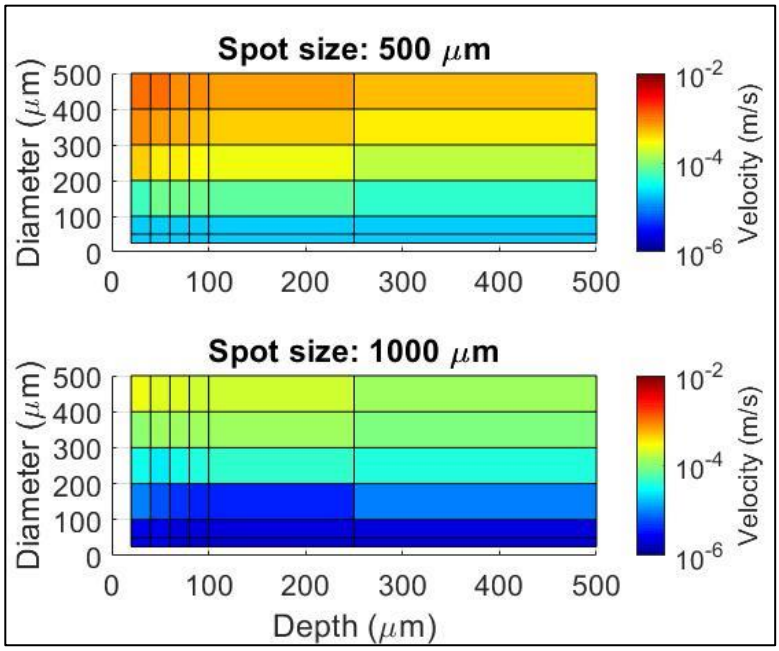

Figure 7: The peak differences in the Rayleigh wave vertical velocity are plotted for each of the spot sizes with respect to the depth and diameter of each pore.

a)

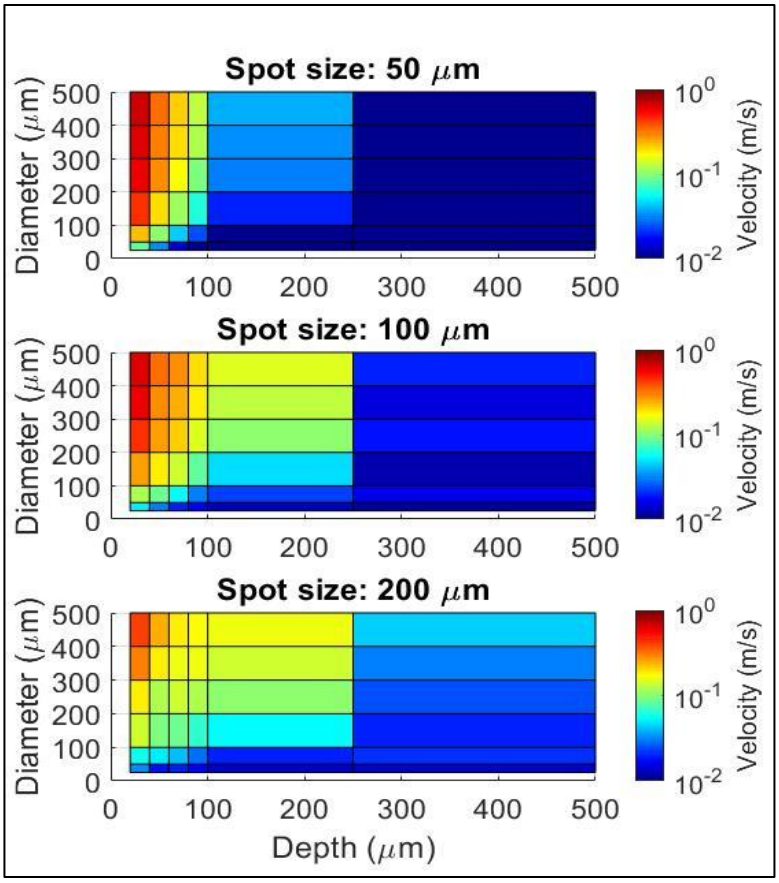

b)

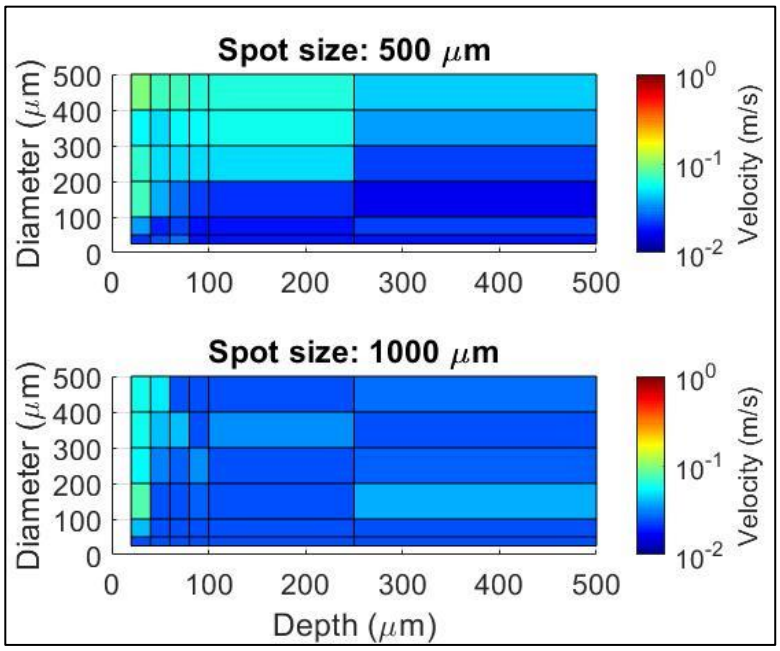

Figure 8: The peak differences in the vertical velocity at the center of the spot are plotted for each spot sizes with respect to the depth and diameter of each pore.

Similar results can be obtained at the center where the laser heating occurs. In regards to the amplitude changes, they are a couple orders larger than the Rayleigh wave. From Figure 8, the changes are better defined near the surface for each pore diameter in comparison to the Rayleigh wave. Using this property and with the time it takes for the ultrasonic wave to reach the pore and return to the surface, it would then make calibration feasible for determining the size of the pore.

3. Experimental Results

In order to determine the effect of the spot size, several different measures were taken to ensure that the parameters of the experiment match the simulation. In particular, the most important one was to determine the beam profile of the laser. In general, the optical specifications are provided by venders. However, since the beam was being focused as a function of distance, this needs to be taken into account. In addition, the beam profiles of lasers can vary depending on the manufacturing, environment, angle of incidence. Fortunately, beam profiling cameras provide an easy solution to this problem. Given the wavelength and power of the laser, a beam splitter, and ND filters were used to scale down the power of the SPI laser and later model the beam profile of the laser system as a function of distance from the source.

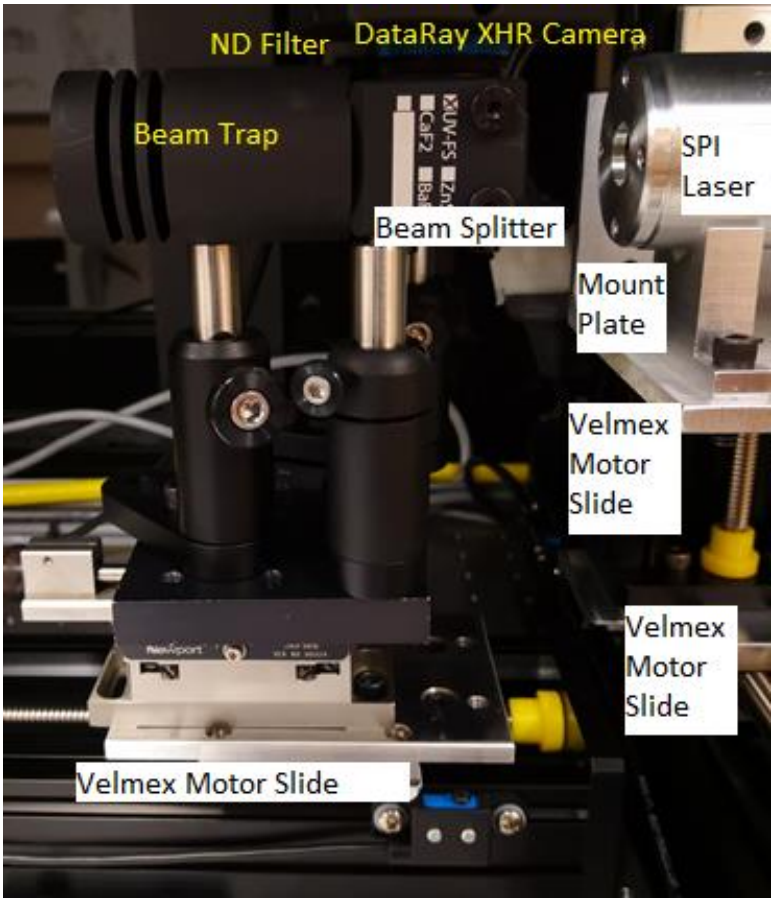

Figure 9: Setup for the beam profiling experiment.

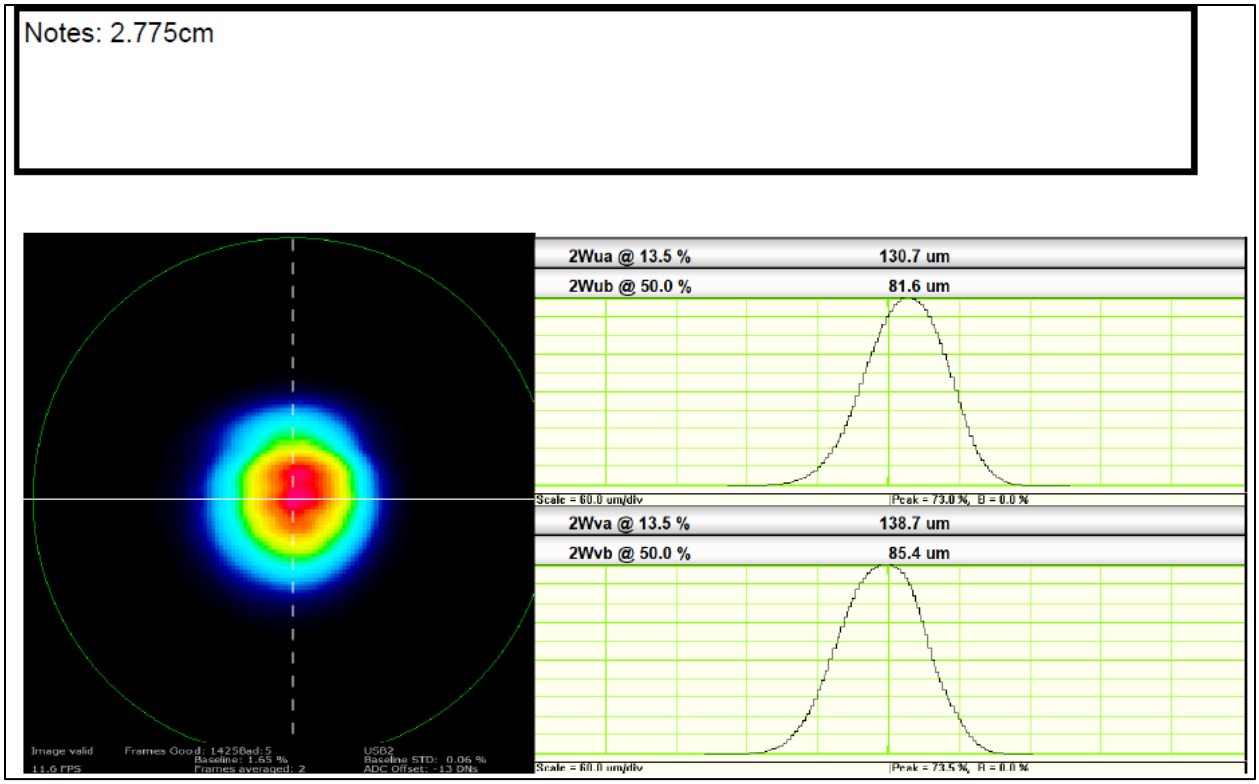

Figure 10: Beam Profile of the 1064nm SPI laser for a given position.

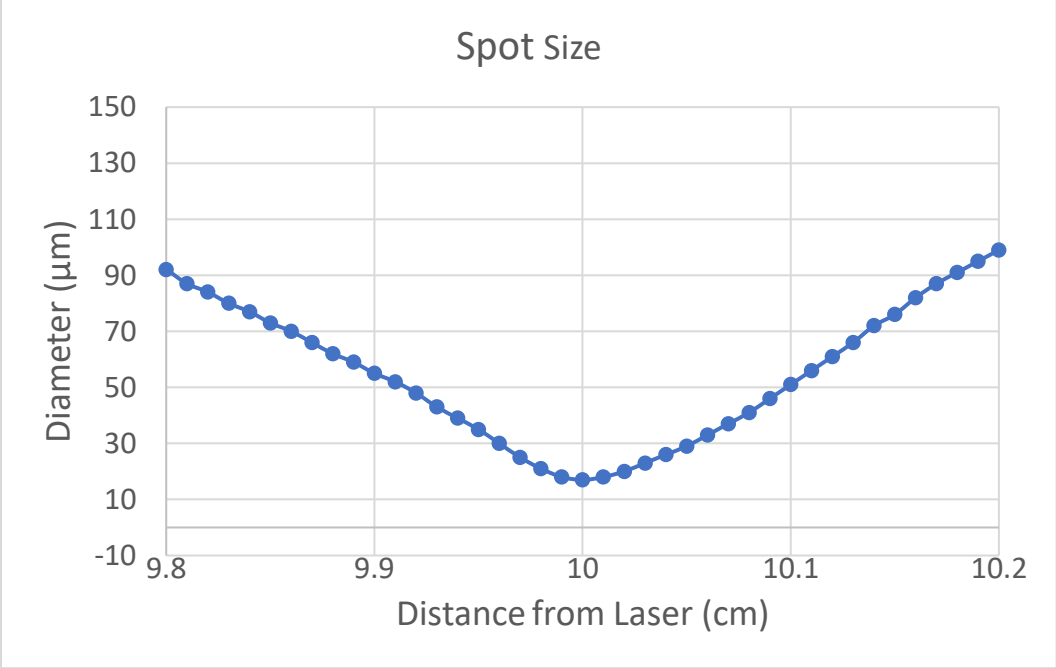

Figure 11: Beam Diameter varied as a function of distance.

From the measurements, it was determined that the minimum spot size was approximately 18μm at the focal length. However, due to the camera specifications, the laser beam profile could only be measured with a pixel resolution of 3.2 μm. This means that the error in the spot diameter will be ±6.4 μm. In addition, errors may be introduced due to alignment of the optical equipment and the laser. Another cause of error would be the accuracy of the distance between the optical equipment and the laser. In addition, modeling the beam width as a function of the distance near the focus was limited by the accuracy of the Velmex motors.

With the measured beam profile as provided in Figure 10 and Figure 11, laser ultrasonic measurements as a function of spot size could now be taken. This was be accomplished using the Optech system. In theory, the system made use of photorefractive crystal and two-wave mixing. To better understand the results, the method the system uses to interpret the measurements was by having two waves interfere with each other while modulating the waves to measure the phase shifts in the waves[8,9]. In the example of a heterodyne interferometer, the intensity measured at the photodiode was[10]

$$I = I_o\left(1 + Mcos(2\pi f_L t + 2k_o\delta \sin(2\pi f_U t))\right). \quad [6]$$

The Optech system has a similar concept. A reference beam and a signal beam are used to measure the displacement using two-wave mixing. The receiver takes care of demodulating the signal and converting it into a voltage value. This measurement on the oscilloscope would then be used in conjunction with a given sensitivity value provided by the manufacturer to interpret the voltage signal into a displacement signal.

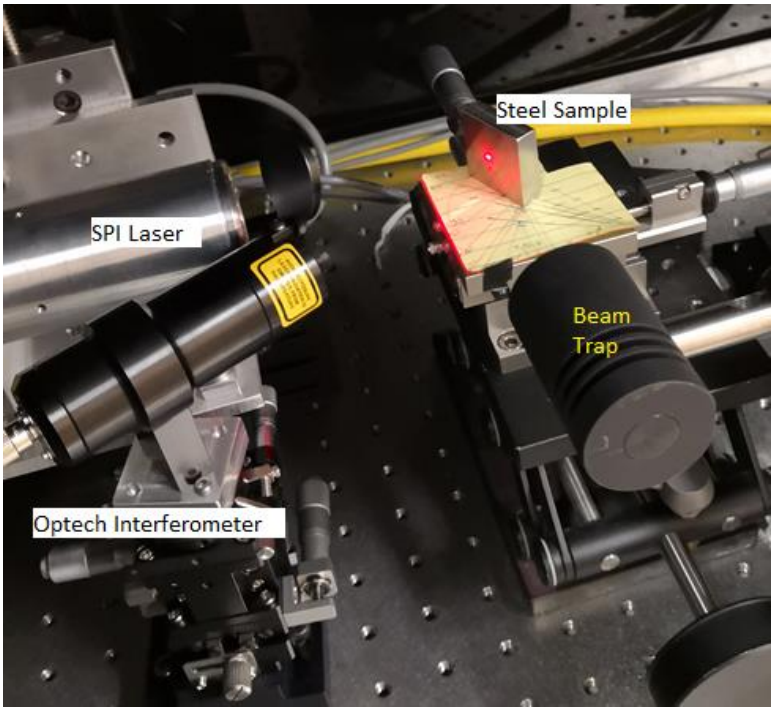

Figure 12: The interferometer was placed normal to the surface of the sample. The SPI laser was set such that the incident light was approximately 30° away from the normal of the interface. In addition, a beam trap was used to help capture any light from the SPI laser that was reflected off the surface.

The system was capable of detecting changes in displacement due to the Rayleigh wave generated by the laser. The signal detected had a waveform as shown in Figure 13. The signals detected were then measured for each spot size in order to determine the frequency response. When detecting the Rayleigh waves, the measured results showed that the strongest ultrasonic waves were by those generated using a smaller spot size. In terms of the frequency of the displacement, the wave did not have a high frequency component. When increasing the power of the laser, it was seen that the frequency content would shift down. In addition, if the laser is allowed to generate more pulses in succession, it would cause the heated surface to enter the ablation region and skewing the desired results.

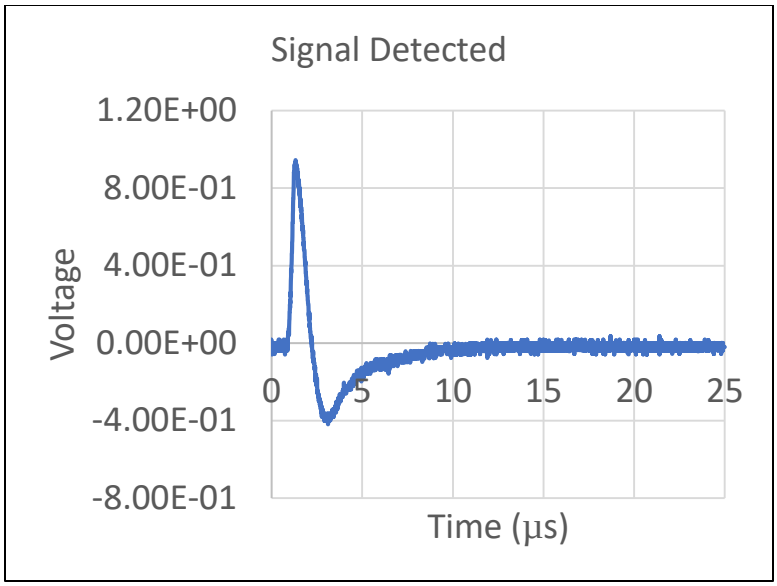

Figure 13: Wave detected using the Optec interferometer for a single pulse of the laser.

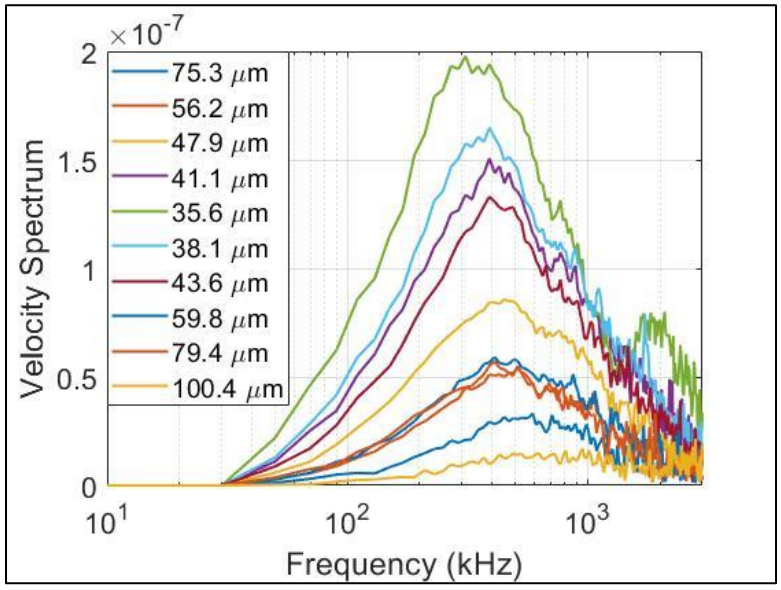

Figure 14: Frequency spectrum for the measured signal detection of the Rayleigh wave.

From the measured spectrum, there was very little to no variation in regards to the frequency of the measured signal. One take away was that as the spot size decreased, the amplitude of the measured Rayleigh wave increased. It should be noted that the frequency content of these waves has likely been limited by the spot size of the detector. The spot size was approximately 0.4mm. This means that if we want to capture the variations of these traveling waves along the surface as

a function of time at a certain point in space, the spatial and temporal resolutions of the receiver system should be relatively small to capture the variations of the traveling wave.

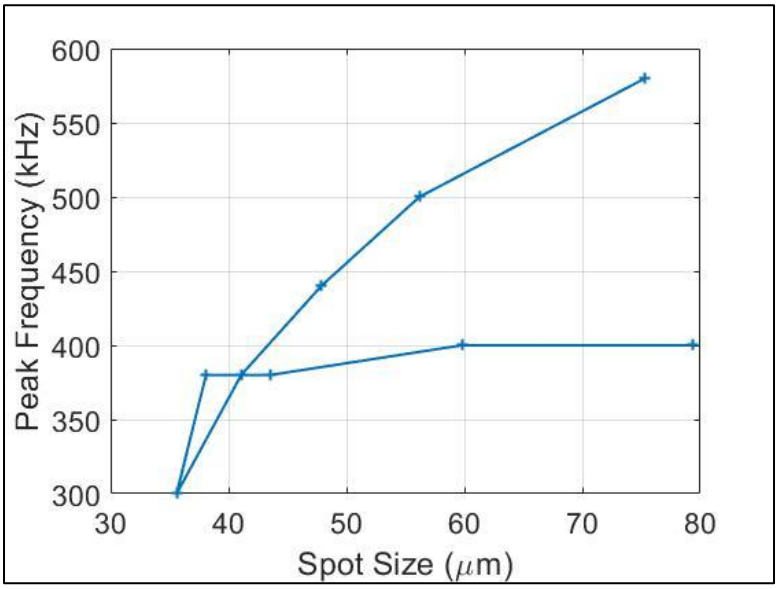

Figure 15: The relationship between spot size and the peak frequency is plotted to determine is a relationship exists. Based on the values, it can be determined that for the given range in spot sizes, there is no definitive relationship between the two.

4. Conclusion

In the work presented, the simulations demonstrated that the effect of changing the spot size of the laser with respect to the ultrasonic wave's peak frequency were inversely proportional to each other. In addition, given that a smaller spot size could generate a wave with a higher frequency, and it was calculated that the measured velocity differences will vary in a controlled manner such that the reflections increased the difference when the spot was either close to the surface or large in diameter. For larger beam spot sizes, the differences were relatively smaller compared to the smaller beam spots. While it was not possible to conduct the experiment as desired, the results did provide some information in regards the amplitude of the waves detected. More specifically, smaller spot sizes generated waves with larger amplitudes.

References

[1] A. Moreau, M. Lord High Frequency Laser-Ultrasonics. In: Green R.E. (eds) Nondestructive Characterization of Materials VIII. Springer, Boston, MA, 1998

[2] A. Valdes, "Development of laser ultrasonic and interferometric inspection system for high-volume on-line inspection of microelectronic devices.", Georgia Institute of Technology, May 2009

[3] A. Blouin, C. Neron, B. Campagne, J.-P. Monchalin, "Applications of Laser-Ultrasonics and Laser-Tapping to Aerospace Composite Structures", 17th World Conference on Nondestructive Testing, 25-28 Oct. 2008, Shanghai, China, Accessed March 2019.

[4] J.P. Mochalin, "Non-Contact Generation and Detection of Ultrasound with Lasers", Industrial Materials-NRC, Boucherville, Quebec, Nov. 2004.

[5] S.O. Kasap, "Optoelectronics & Photonics: Principles & Practices", 2nd ed, 2013

https://ieeexplore-ieee-org.proxy.lib.iastate.edu/document/6725137

[6] S.-L. Chen, "Review of Laser-Generated Ultrasound Transmitters and Their Applications to All-Optical Ultrasound Transducers and Imaging", MDPI, 2016

[7] Jonathan R. Fincke, Charles M. Wynn, Rob Haupt, Xiang Zhang, Diego Rivera, Brian Anthony, "Characterization of laser ultrasound source signals in biological tissues for imaging applications," J. Biomed. Opt. 24(2) 021206 (8 December 2018)

[8] J. Ke, C. Duan, W. Yi, and C. Yan, "Application of an Adaptive Two-wave Mixing Interferometer for Detection of Surface Defects," 2016 Progress In Electromagnetic Research Symposium, 2016

[9] N. Koukourakis, T. Abdelwahab, M. Y. Li, H. Höpfner, Y. W. Lai, E. Darakis, C. Brenner, N. C. Gerhardt, and M. R. Hofmann, "Photorefractive two-wave mixing for image amplification in digital holography," Opt. Express 19, 22004-22023 (2011)

[10] B. F. Pouet, R. K. Ing, S. Krishnaswamy, D. Royer, "Heterodyne interferometer with two-wave mixing in photorefractive crystals for ultrasound detection on rough surfaces." American Institute of Physics. S0003-6951(96)02151-1. 1996